Journal of Neuroimmunology 331 (2019) 46–57

Contents lists available at ScienceDirect

Journal of Neuroimmunology

journal homepage: www.elsevier.com/locate/jneuroim

The control of oligodendrocyte bioenergetics by interferon-gamma (IFN-γ) and Src homology region 2 domain-containing phosphatase-1 (SHP-1)

Scott B. Minchenberg[a], Paul T. Massa[a,b,*]

[a] Department of Microbiology and Immunology, SUNY Upstate Medical University, 750 East Adams Street, Syracuse, NY, United States
[b] Department of Neurology, SUNY Upstate Medical University, 750 East Adams Street, Syracuse, NY, United States

ARTICLE INFO

Keywords:
Cytokine signaling
Interferon gamma [IFN-γ]
SHP-1 [PTPN6]
Glycolysis
Mitochondria
Metabolism

ABSTRACT

Glycolysis and mitochondrial respiration are essential for oligodendrocyte metabolism in both the developing and adult CNS. Based on recent reports on the effects of the proinflammatory cytokine IFN-γ on metabolism and on oligodendrocytes, we addressed whether IFN-γ may affect oligodendrocyte bioenergetics in ways relevant to CNS disease. Oligodendrocytes of mice treated with IFN-γ showed significant reductions in aerobic glycolysis and mitochondrial respiration. As expected, IFN-γ treatment led to the induction of STAT1 in oligodendrocytes indicating active signaling into these cells. To determine the direct effects of IFN-γ on oligodendrocyte metabolism, cultured oligodendrocytes were treated with IFN-γ *in vitro*, which resulted in suppression of glycolysis similar to oligodendrocytes of animals treated with IFN-γ *in vivo*. Mice lacking SHP-1, a key regulator of IFN-γ and STAT1 signaling in CNS glia, had high constitutive levels of STAT1 and decreased aerobic glycolysis and mitochondrial respiration rates relative to wild type mouse oligodendrocytes. Together, these data show that IFN-γ and SHP-1 control oligodendrocyte bioenergetics in ways that may relate to the role of this cytokine in CNS disease.

1. Introduction

Oligodendrocyte bioenergetics is an area of active research, in which abnormalities in glycolysis or oxidative phosphorylation (OXPHOS) have been implicated in various processes associated with oligodendrocyte and neuronal dysfunction (Amaral et al., 2013; Funfschilling et al., 2012; Saab et al., 2013). The latter studies demonstrated that glial cells are highly glycolytic even under normoxic conditions. In particular, oligodendrocytes, which make extensive contact with axons to provide electrical insulation necessary for saltatory conduction, have been shown to provide lactate from glycolysis as metabolic fuel for axonal mitochondria (Lee et al., 2012; Rinholm et al., 2011).

In addition to maintaining the high-energy demands of axons, glycolysis and OXPHOS are required to meet the unique metabolic demands of oligodendrocytes. When actively myelinating, oligodendrocytes have a high bioenergetic demand and require both mitochondrial and glycolytic metabolism to allow for the synthesis of the myelin sheathes (Funfschilling et al., 2012; Ziabreva et al., 2010). Adequate mitochondrial function is particularly important during myelination, and diminished oligodendrocyte mitochondrial function is associated with hypomyelination and axonal degeneration (Andrews et al., 2005; Bjartmar and Trapp, 2001; Mahad et al., 2009; Takikita et al., 2015). After myelination is complete, oligodendrocytes can maintain myelin by utilizing glycolysis independently from mitochondrial respiration (Funfschilling et al., 2012). Recently, it has been reported that downregulation of glycolysis in cultured primary oligodendrocytes triggers process withdrawal, a mechanism oligodendrocytes might utilize to conserve energy in an effort to prevent apoptosis due to bioenergetics failure *in vivo* (Rone et al., 2016). Thus, both glycolytic and mitochondrial metabolism are essential in the context of myelination and axonal bioenergetics, and the pathways regulating these processes are critical for oligodendrocyte function and survival.

In the human demyelinating disease, multiple sclerosis (MS), oligodendrocytes may be direct targets for immune-mediated damage leading to subsequent demyelination. In this regard, extensive research has been conducted on the effects IFN-γ on oligodendrocyte biology and demyelination. IFN-γ is a proinflammatory cytokine that is relevant in the context of inflammatory demyelination since IFN-γ is produced by

Abbreviations: 2-DG, (2-deoxyglucose); ECAR, (extracellular acidification rate); ETC, (electron transport chain); FCCP, (carbonyl cyanide-4-(trifluoromethoxy)phenylhydrazone); iNOS, (inducible nitric oxide synthase); LIF, (leukemia inhibitory factor); MCT, (monocarboxylate transporter); me/me, (motheaten); NO, (nitric oxide); OCR, (oxygen consumption rate); OXPHOS, (oxidative phosphorylation); PV, (pervanadate); R/AA, (rotenone/antimycin A); SHP-1, (src homology region 2 domain-containing phosphatase-1); WT, (wild type)

* Corresponding author.
E-mail address: MassaP@upstate.edu (P.T. Massa).

http://dx.doi.org/10.1016/j.jneuroim.2017.10.015
Received 17 August 2017; Received in revised form 17 October 2017; Accepted 24 October 2017

and mediates demyelinating activity by encephalitogenic T-cells in autoimmune models of MS (Balabanov et al., 2007; Goverman, 2009; Lees and Cross, 2007; Lin et al., 2007; Loda and Balabanov, 2012; Renno et al., 1998) and is produced by anti-viral T cells important for antiviral activities and cell death of oligodendrocytes in viral models of demyelination(Bergmann et al., 2003; De-Simone et al., 2015; Gonzalez et al., 2005; Parra et al., 2010; Schijns et al., 1991; Tsunoda et al., 2006). An important aspect of these studies on IFN-γ using these models is that both detrimental and beneficial outcomes have been reported which is not currently understood (Lin et al., 2006; Sosa et al., 2015; Vartanian et al., 1995; Willenborg et al., 1996). In this regard, IFN-γ acts on oligodendrocytes to induce STAT1 homodimers, a major component of proinflammatory, antiviral, and bioenergetic signaling (Agresti et al., 1998; Boehm et al., 1997; Decker et al., 1997). We propose that as found in other cells, that STAT1 acts to modulate bioenergetics in oligodendrocytes and is critical to the activity of IFN-γ on oligodendrocytes.

There are multiple regulators of IFN-γ signaling that are likely to have profound effects on responsiveness in oligodendrocytes. One in particular is the protein tyrosine phosphatase SHP-1, which has been shown to negatively regulate IFN-γ activity in multiple tissues and cell types (Shuai and Liu, 2003; Starr and Hilton, 1999; Valentino and Pierre, 2006). SHP-1 is a major regulator of IFN-γ signaling in CNS glia (Massa et al., 2000; Massa and Wu, 1996), however whether SHP-1 controls IFN-γ responsiveness in oligodendrocytes is unknown. Of particular interest in this regard, SHP-1-deficient (motheaten, me/me) mice display a significant degree of oligodendrocyte pathology (Wishcamper et al., 2001), dysmyelination (Massa et al., 2004) and astrocytosis (Horvat et al., 2001), consistent with a role for SHP-1, IFN-γ, and STAT1 activity in oligodendrocyte biology (Gruber et al., 2015; Massa et al., 2000). The main question in the present studies is whether these responses to IFN-γ may be coincident with alteration in oligodendrocyte bioenergetics. Our findings suggest that IFN-γ STAT1, and SHP-1 signaling in oligodendrocytes induces metabolic alterations in oligodendrocytes that are related to mechanisms of oligodendrocyte pathology and demyelinating disease.

2. Materials & methods

2.1. Animals

SHP-1-deficient mice (motheaten locus, me/me) on a C3HeB/FeJLe-a/a background (RRID:IMSR_JAX:000225) and phenotypically normal littermates (wild type, WT) were produced from heterozygous breeding pairs obtained from Jackson Laboratories (Bar Harbor, ME). The strain designation for heterozygous breeders for motheaten mice is C3FeLe.B6 a/a-Ptpn6me/J (stock no. 000225). Both male and female mice were used throughout studies described below. All animal procedures were approved by the Institutional Animal Care and Use Committee at SUNY Upstate Medical University in compliance with the National Institutes of Health Guide for Care and Use of Laboratory Animals.

2.2. Isolation of oligodendrocytes from the mouse CNS

Wild type and motheaten mice that were 7- or 8- days old were perfused with 20 mL of phosphate buffered saline (PBS) or PBS with 100 μM sodium pervanadate, pH 7.4. Brains and spinal cords of 7- or 8-day-old wild type and motheaten mice were dissociated using a neural tissue dissociation kit (Miltenyi Biotec, San Diego, CA) according to the manufacturer's instructions, and oligodendrocytes were purified using O4 antibody conjugated to magnetic beads. The O4-positive oligodendrocytes were passed through a magnetic column on a QuadroMACS™ Separator (Miltenyi Biotec, San Diego, CA) to remove unlabeled glia and neurons. Although the resulting O4-isolated population displayed characteristic morphological criteria of oligodendrocytes by phase contrast microscopy (rounded cell bodies with multiple fine caliber processes) (Massa et al., 2000), immunofluorescence staining of this preparation for the oligodendrocyte marker myelin basic protein (MBP) showed that only about half the cells were positive(Supplemental data, Fig. 1). We concluded based on these observations that O4-positive cells isolated from P7 animals represent a heterogeneous mixture of both mature MBP + oligodendrocytes and less mature MBP-negative cells that may be oligodendrocyte progenitor cells (OPC). However, we refer to these preparations simply as oligodendrocytes.

2.3. Western immunoblots

Whole-cell extracts were prepared as previously described (Massa et al., 2004). Cells or tissues were homogenized in RIPA buffer. 50 to 100 micrograms of protein per lane was electrophoresed through a 10% or 12% polyacrylamide resolving gel and electroblotted to a polyvinylidene difluoride membrane (Millipore, Billerica, MA). Membranes were blocked with 5% bovine serum albumin for 1 h, and then incubated with one of the following primary antibodies: Y701-pSTAT1 (Cell Signaling Technology Cat# 9167S RRID:AB_561284), total STAT1 (Cell Signaling Technology Cat# 9172 RRID:AB_2198300), Y705-pSTAT3 (Cell Signaling Technology Cat# 9145 also 9145S, 9145P, 9145L RRID:AB_2491009), total STAT3 (Cell Signaling Technology Cat# 12640 also 12640S RRID:AB_2629499), GAPDH (Cell Signaling Technology Cat# 5174 also 5174P, 5174S RRID:AB_10622025), or actin (Abcam Cat# ab3280 RRID:AB_303668), followed by HRP-conjugated IgG secondary antibody (DAKO Corporation, Carpinteria, CA). Enhanced chemiluminescence (Amersham Life Sciences, Cleveland, OH) was used to visualize reactive protein bands on the ChemiDOC, and quantified using the Image Lab software (Bio-Rad, Hercules, CA).

2.4. In Vivo treatment of mice with cytokines

P6-8 wild type and motheaten mice were injected I.P. with 100 μL of IFN-γ (R & D Systems, Minneapolis, MN) in PBS with 0.5% BSA at a concentration of 100 U/g body weight. PBS with 0.5% BSA was used as a vehicle control and injected at a volume of 100 μL. After 24 h of cytokine treatment, the brains and spinal cords were removed and the $O4^+$ oligodendrocytes were isolated and analyzed as outlined above.

2.5. In vivo metabolic analysis

Oligodendrocytes freshly isolated from wild type and motheaten mouse brains and spinal cords were plated on Seahorse XF^e96 cell culture microplates (Agilent, Santa Clara, CA) that were pretreated for 20 min with Cell-Tak (Corning Inc., Corning, NY) at a concentration of 3.5 μg Cell-Tak/cm^2 of surface area. The oligodendrocytes were plated at a density of 200,000 live cells per well and incubated in 175 μL of XF Base media (Agilent, Santa Clara, CA) with 2 mM glutamate at a pH of 7.4 for analysis of glycolysis or in 175 μL of XF base media (Agilent, Santa Clara, CA) with 25 mM glucose, 2 mM glutamate, and 1 mM pyruvate at a pH of 7.4 for analysis of mitochondrial function. The cells were incubated at 37°C for 1 h and were analyzed using the Seahorse XF^e96 Analyzer. Four cycles were performed which consisted of 3 min of mixing followed by three minutes of measuring. For measuring glycolysis, the basal extracellular acidification rate (ECAR) was measured in the first cycle. After the first cycle was completed, 25 μL of glucose was injected so that the working concentration was 10 mM and the second cycle measured the changes in ECAR after the introduction of glucose. After the second cycle was completed, 25 μL of the ATPase inhibitor oligomycin was injected (final concentration, 2 μM). Finally, 2-deoxy-D-glucose (2-DG) was injected to a final concentration of 50 mM. The rate of basal glycolysis was determined by subtracting the ECAR before the glucose injection from the ECAR after the glucose injection. The glycolytic capacity was determined by subtracting the ECAR after glucose injection from the ECAR after the oligomycin injection. A schematic diagram illustrating this analysis is shown in

Supplementary Fig. 2.

For quantifying alterations in mitochondrial metabolism, the basal oxygen consumption rate (OCR) was measured followed by a 25 μL injection of oligomycin to give a final oligomycin concentration of 2 μM, a second 25 μL injection of carbonyl cyanide-4-(trifluoromethoxy)phenylhydrazone (FCCP) (final concentration of 2 μM), and a third 25 μL injection of rotenone/antimycin A to give a final concentration of 0.5 μM. The basal mitochondrial oxygen consumption was calculated by subtracting the OCR independent of mitochondrial function (OCR measured after rotenone/antimycin A injection) from the basal OCR of the cell. The maximal mitochondrial respiration was measured by subtracting the OCR obtained after rotenone/antimycin A injection from the OCR after FCCP treatment. The mitochondrial ATP production was calculated by subtracting the basal oxygen consumption from the oxygen consumption after oligomycin treatment. Finally, the spare respiratory capacity was calculated by subtracting the OCR after FCCP treatment from the basal cellular OCR. A schematic diagram illustrating this analysis is shown in Supplementary Fig. 2. The metabolic data for the oligodendrocytes were analyzed using the Wave software (Agilent, Santa Clara, CA). The cell loading was standardized to GAPDH levels in oligodendrocytes isolated from each group since IFN-γ treatment and genotype did not have any significant effect on oligodendrocyte GAPDH levels.

2.6. In vitro cytokine treatments and oligodendrocyte cultures

Oligodendrocytes from P6-P8 mice were isolated from wild type as outlined above. The oligodendrocytes were plated on Seahorse XF^{e}96 cell culture microplates (Agilent, Santa Clara, CA) that were pretreated for 20 min with Cell-Tak (Corning Inc., Corning, NY) at a concentration of 3.5 μg Cell-Tak/cm^2 of surface area. The oligodendrocytes were cultured for 24 h in complete culture medium containing Dulbecco's modified Eagle's medium (DMEM, Gibco, Carlsbad, CA), 10% FBS (Gibco, Carlsbad, CA), 100 U/mL of penicillin, 100 μg/mL of streptomycin, and 0.5% BSA in PBS, 100 U/mL of IFN-γ (R & D Systems, Minneapolis, MN), or 100 U/mL of LIF R & D Systems, Minneapolis, MN).

2.7. In vitro metabolic analysis

After 24 h in culture, the culture media was washed and replaced with 175 μL of XF Base media (Agilent, Santa Clara, CA) with 10 mM glucose and 2 mM glutamate at a pH of 7.4 for analysis of glycolysis or in 175 μL of XF base media (Agilent, Santa Clara, CA) with 25 mM glucose, 2 mM glutamate, and 1 mM pyruvate at a pH of 7.4 for analysis of mitochondrial function. The cells were incubated at 37C° for one hour and were analyzed using the Seahorse XF^{e}96 Analyzer as described above.

The rate of basal glycolysis was determined by subtracting the average ECAR after 2-DG injection from the average ECAR after the glucose injection. The glycolytic capacity was determined by subtracting the average ECAR after glucose injection from the average ECAR after the oligomycin injection.

The basal mitochondrial oxygen consumption was calculated by subtracting the average OCR independent of mitochondrial function (OCR measured after rotenone/antimycin A injection) from the average basal OCR of the oligodendrocytes. The maximal mitochondrial respiration was measured by subtracting the average OCR obtained after rotenone/antimycin A injection from the average OCR after FCCP treatment. The mitochondrial ATP production was calculated by subtracting the average basal oxygen consumption from the average oxygen consumption after oligomycin treatment. Finally, the spare respiratory capacity was calculated by subtracting the average OCR after FCCP treatment from the average basal cellular OCR. The metabolic data for the oligodendrocytes were analyzed using the Wave software (Agilent, Santa Clara, CA). The cell loading was standardized using CyQUANT to account for alterations in cell viability.

2.8. Statistical analysis

Histograms and tables show the mean values with standard error of the mean. The numbers of samples or individual mice used in each assay are indicated in the figure legends. For comparisons between two samples, *p*-values were generated using the unpaired Student's *t*-test. For comparisons between more than two samples, statistical significance was determined by an ANOVA. The particular test used for each experiment is indicated in the figure legends. A p-value of < 0.05 was interpreted as statistically significant. All statistical analyses were performed using Graphpad Prism (version 7).

3. Theory

The cytokine IFN-γ has been shown to have multiple important biological activities in oligodendrocytes ranging from increased expression of immune molecules, cell death induction, and anti-viral state. Recently, the role of specific bioenergetic pathways in these IFN-γ responses has been discovered. Therefore, the role of IFN-γ in altering the bioenergetic state of oligodendrocytes may provide important mechanistic insights into how IFN-γ acts on oligodendrocytes in health and disease.

4. Results

4.1. Treatment of mice with IFN-γ suppresses oligodendrocyte glycolytic and mitochondrial metabolism

Previous studies have demonstrated that IFN-γ regulates bioenergetics in many cell types (Karhumaki and Helin, 1987; Su et al., 2015) and IFN-γ signaling is relevant to mechanisms of oligodendrocyte pathology and inflammatory demyelination in MS. Of particular relevance to oligodendrocyte viability and myelination is glycolytic and mitochondrial respiration (Rone et al., 2016). To determine the effects of IFN-γ on wild type mouse oligodendrocyte bioenergetics *in vivo*, we treated wild type mice with IFN-γ for 24 h and conducted metabolic studies on freshly isolated oligodendrocytes from brain and spinal cord. Oligodendrocytes of mice treated with IFN-γ for 24 h displayed both decreased basal aerobic glycolysis and glycolytic capacity (Fig. 1A–C; Supplementary Fig. 2). Moreover, oligodendrocytes from IFN-γ-treated wild type mice had significantly reduced parameters of mitochondrial metabolism including basal mitochondrial oxygen consumption, maximal mitochondrial respiration, ATP production, and spare respiratory capacity relative to untreated wild type mice (Fig. 1D–H, Supplementary Fig. 2). Trypan blue staining revealed no alterations in oligodendrocyte viability after *in vivo* IFN-γ treatment relative to oligodendrocytes isolated from untreated animals (data not shown). Overall, we demonstrated that IFN-γ significantly reduced oligodendrocyte glycolytic and mitochondrial metabolism.

4.2. Direct effects of IFN-γ on oligodendrocyte metabolism

Based on the effects of IFN-γ on oligodendrocyte bioenergetics *in vivo*, we wanted to determine if IFN-γ could act directly on oligodendrocyte bioenergetics. To determine the direct effects of IFN-γ on oligodendrocyte metabolism, freshly isolated oligodendrocytes from brain and spinal cord were cultured for 24 h in the presence of IFN-γ prior to metabolic analysis. IFN-γ significantly reduced basal glycolysis and glycolytic capacity (Fig. 2A–C), a finding that agreed with effects of *in vivo* IFN-γ treatment (Fig. 1A–C). However, in contrast to *in vivo* treatment, *in vitro* treatment with IFN-γ significantly increased basal mitochondrial oxygen consumption (Fig. 2D,E) but had no effect on maximal mitochondrial respiration, mitochondrial ATP production, or spare respiratory capacity (Fig. 2D,F–H). This suggests that IFN-γ

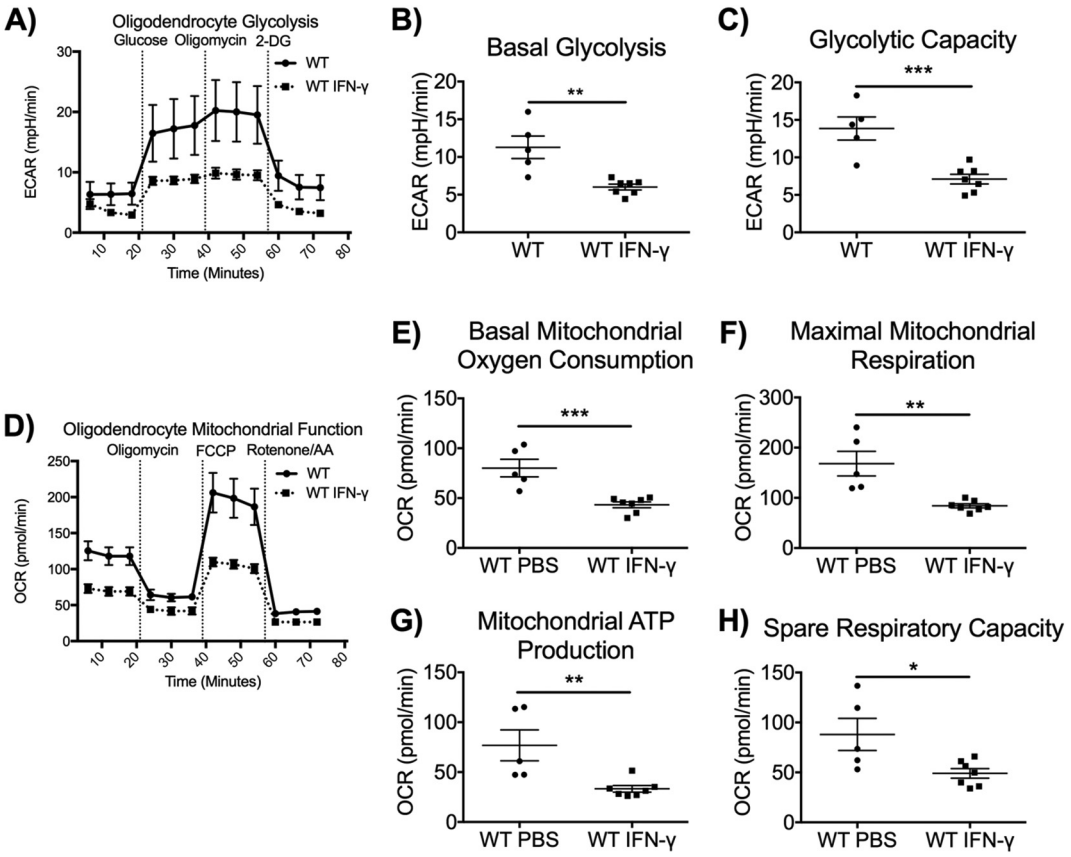

Fig. 1. Constitutive and *in vivo* IFN-γ treated wild type mouse oligodendrocyte metabolism. A) Seahorse extracellular flux analyzer graph depicting the change in extracellular acidification (ECAR) over time for oligodendrocytes isolated from untreated wild type (WT) mice, and from mice injected IP with IFN-γ for 24 h (WT n = 5, WT IFN-γ n = 7). B & C) Scatter plot graphs depicting B) basal glycolysis (p = 0.0013; WT n = 5, WT IFN-γ n = 7) and C) glycolytic capacity (p = 0.0005; WT n = 5, WT IFN-γ n = 7) of oligodendrocytes from untreated WT mice and WT mice treated with IFN-γ. D) Seahorse extracellular flux analyzer graph depicting the oxygen consumption rate (OCR) over time for oligodendrocytes isolated from untreated WT mice and WT mice treated with IFN-γ (WT n = 5, WT IFN-γ n = 7). E–H) Scatter plot graphs depicting E) basal mitochondrial oxygen consumption (p = 0.0005; WT n = 5, WT IFN-γ n = 7), F) maximal mitochondrial respiration (p = 0.0012; WT n = 5, WT IFN-γ n = 7), G) ATP production (p = 0.0044; WT n = 5, WT IFN-γ n = 7), and H) spare respiratory capacity (p = 0.0114; WT n = 5, WT IFN-γ n = 7) of oligodendrocytes isolated from untreated and IFN-γ treated mice. Graphs depict oligodendrocytes isolated from the brains and spinal cords of P6–P8 mice, standardized to GAPDH levels to control for cell numbers between samples. Each data point represents oligodendrocytes derived from a single mouse and significance was determined by unpaired one-tailed Student's *t*-test (*p < 0.05, **p < 0.01, ***p < 0.001). Glycolytic capacity is the maximal rate the cell can perform glycolysis and is closely related to the expression level of glycolytic enzymes in the cell. This differs from basal glycolysis which is influenced by other factors, mainly mitochondrial ATP production. Maximal mitochondrial respiration is the maximal rate the mitochondria can consume oxygen and is related to the expression and posttranslational modification of complexes in the ETC in the oligodendrocytes. This differs from basal mitochondrial oxygen consumption which is regulated by various factors, mainly glycolytic ATP production. A description of different Seahorse measurements and conditions under which measurements are made is shown in Supplementary Fig. 1.

directly impacts oligodendrocyte glycolysis, whereas the effects on mitochondrial function on oligodendrocyte mitochondria may be indirect, potentially involving other factor(s)/cell type(s) present *in vivo*.

4.3. Activation of STAT1 in oligodendrocytes by IFN-γ

To determine whether IFN-γ treatment was signaling in oligodendrocytes, *in vivo*- and *in vitro*-treated oligodendrocytes were analyzed by western immunoblot for STAT1, as IFN-γ is a major stimulus of STAT1 phosphorylation, activation, and positive STAT1 gene autoregulation (Boehm et al., 1997; Decker et al., 1997). Thus, IFN-γ treatment of mice and oligodendrocyte cultures led to a significant induction of STAT1 tyrosine phosphorylation (Fig. 3A,C) that is known to be critical for activation of STAT1 transcriptional activity. The latter was consistent with the induction of total STAT1 protein in oligodendrocytes by IFN-γ treatment by autoregulation (Fig. 3A,C). Since STAT3 activation is known to elicit metabolic changes (Meier and Larner, 2014; Poli and Camporeale, 2015; Sarafian et al., 2010; Wegrzyn et al., 2009), the levels of Y705-pSTAT3 were quantified as a control for possible cross talk between signal transduction pathways. IFN-γ treatment in mice and in oligodendrocyte cultures elicited no significant changes in the induction of Y705-pSTAT3 or total STAT3 in oligodendrocytes (Fig. 3B,D). Taken together, these data show that both *in vivo* and *in vitro* IFN-γ treatment activated STAT1 but had no effects on STAT3 activation in oligodendrocytes.

4.4. Regulation of STAT1 by SHP-1 in oligodendrocytes

Since IFN-γ activates STAT1 which may relate to changes in bioenergetics, we quantified the constitutive and IFN-γ-inducible activation of STAT1 in wild type and SHP-1-deficient (motheaten, me/me) oligodendrocytes. Regulation of STAT1 activity by SHP-1 in oligodendrocytes would be consistent with the regulation of STAT1 activity described in primary cultured astrocytes in response to IFN-γ stimulation (Massa and Wu, 1996). An additional rationale for this analysis was based on previous reports of SHP-1 expression in oligodendrocytes and oligodendrocyte pathology in me/me mice that might be related to expected bioenergetic suppression (Massa et al., 2000; Massa et al., 2004). As a measure of relative STAT1 activity between genotypes, we analyzed the expression of total STAT1, as STAT1 levels reflect STAT1-mediated transcriptional autoregulation (Boehm et al., 1997; Decker et al., 1997; Wong et al., 2002). Oligodendrocytes isolated from SHP-1-deficient mice constitutively expressed significantly more total STAT1 relative to oligodendrocytes of wild type mice indicating a significantly

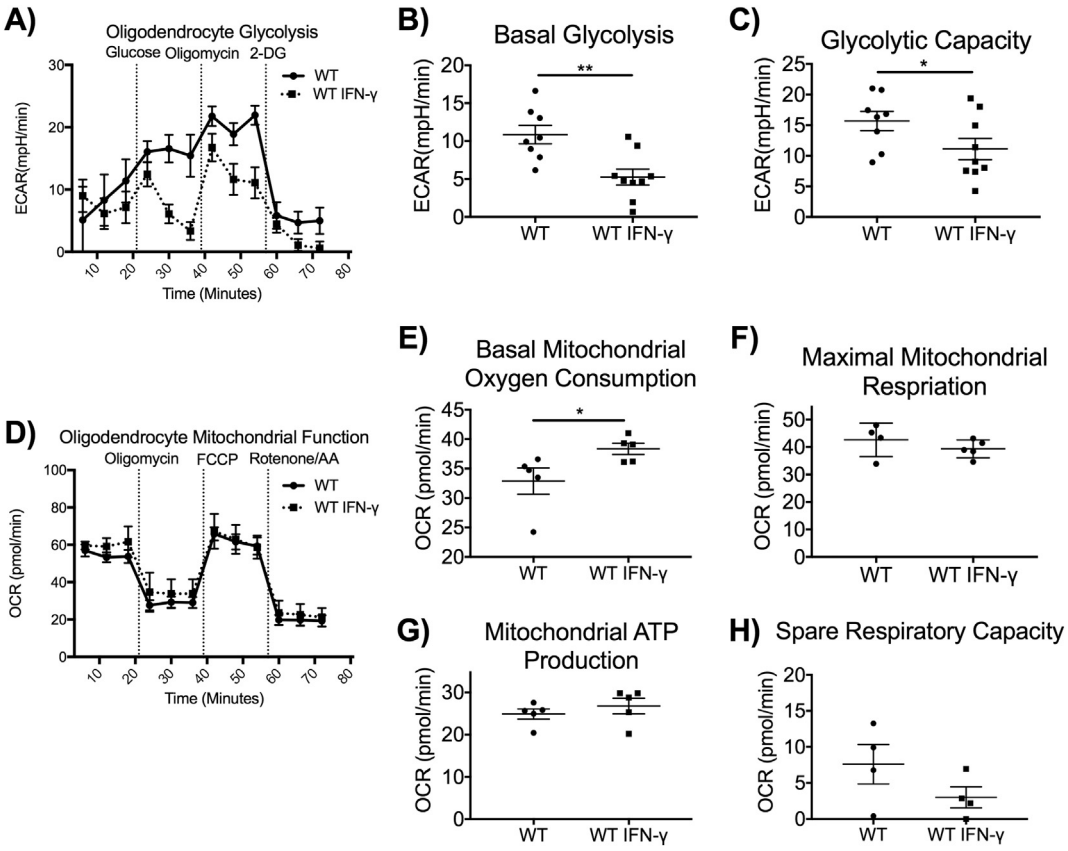

Fig. 2. Glycolytic and mitochondrial metabolism of wild type oligodendrocytes treated *in vitro* with IFN-γ. A) Seahorse extracellular flux analyzer graph depicting the change in extracellular acidification (ECAR) over time for oligodendrocytes isolated from wild type (WT) mice and treated *in vitro* with PBS (control) or 100 U/mL IFN-γ for 24 h (WT n = 8, WT IFN-γ n = 9). B & C) Scatter plot graphs depicting B) basal glycolysis ($p = 0.0016$; WT n = 8, WT IFN-γ n = 9) and C) glycolytic capacity ($p = 0.0360$; WT n = 8, WT IFN-γ n = 9) of oligodendrocytes from WT mice treated *in vitro* with PBS or IFN-γ. D) Seahorse extracellular flux analyzer graph depicting the oxygen consumption rate (OCR) over time for oligodendrocytes isolated from WT mice treated *in vitro* with either PBS (control) or IFN-γ for 24 h (WT n = 4, WT IFN-γ n = 4). E-H) Scatter plot graphs depicting E) basal mitochondrial oxygen consumption ($p = 0.0268$; WT n = 5, WT IFN-γ n = 5), F) maximal mitochondrial respiration ($p = 0.1650$; WT n = 4, WT IFN-γ n = 5), G) ATP production ($p = 0.2075$; WT n = 5, WT IFN-γ n = 5), and H) spare respiratory capacity ($p = 0.3299$; WT n = 4, WT IFN-γ n = 4) of oligodendrocytes isolated from WT mice treated *in vitro* with PBS or WT IFN-γ. Graphs depict oligodendrocytes isolated from the brains and spinal cords of P7 mice, standardized to CyQUANT to control for cell number between samples. Each data point represents individual replicates of oligodendrocytes pooled together from multiple WT mice and significance was determined by unpaired one-tailed Student's *t*-test (*$p < 0.05$, **$p < 0.01$).

higher level of STAT1 activity (Fig. 4A). To the contrary, oligodendrocytes from SHP-1-deficient mice expressed similar amounts of Y705-pSTAT3 and total STAT3 compared to wild type mice (Fig. 4B). To demonstrate a role for SHP-1 as a negative regulator of IFN-γ signaling in oligodendrocytes, we quantified the induction of Y701-pSTAT1 and total STAT1 after *in vitro* IFN-γ treatment of wild type and SHP-1-deficient oligodendrocytes. After 24 h of IFN-γ stimulation, both wild type and motheaten mouse oligodendrocytes had a significant induction of both Y701-pSTAT1 and total STAT1 (Fig. 4C–E), however IFN-γ induced significantly more Y701-pSTAT1 and total STAT1 in SHP-1-deficient oligodendrocytes (Fig. 4C–E) demonstrating a direct role for SHP-1 in the regulation of the STAT1 response to IFN-γ. To show specificity of IFN-γ-mediated activation of STAT1 in oligodendrocytes (*i.e.* crosstalk between signaling pathways) we treated wild type and SHP-1-deficient oligodendrocytes *in vitro* with leukemia inhibitory factor (LIF) which resulted in no observable induction of STAT1 in either wild type or motheaten oligodendrocytes (Fig. 4E). In sum, our data indicate a critical role for SHP-1 in controlling STAT1 activation in oligodendrocytes.

4.5. SHP-1 controls constitutive glycolytic and mitochondrial metabolism

After observing that IFN-γ downregulated metabolism in oligodendrocytes of wild type mice, we wanted to determine if oligodendrocytes of SHP-1-deficient mice displayed constitutively depressed bioenergetics compared to wild type oligodendrocytes. We believed that this was a distinct possibility as these SHP-1-deficient cells exhibited an abnormally heightened STAT1 activation independently of IFN-γ (Fig. 4A) as previously seen in SHP-1-deficient macrophages (David et al., 1995). As expected, oligodendrocytes isolated from SHP-1-deficient mice had a significant reduction in both basal glycolysis and glycolytic capacity relative to wild type oligodendrocytes (Fig. 5A–C). As well, we observed a significant decrease in basal mitochondrial oxygen consumption, maximal mitochondrial respiration, ATP production, and spare respiratory capacity (Fig. 5D–H) consistent with data obtained from oligodendrocytes of IFN-γ-treated wild type mice (Fig. 1A–H). It is important to note that there were no differences in viability between wild type and SHP-1-deficient mouse oligodendrocytes as determined by trypan blue staining (data not shown). Taken together, these data showed that loss of SHP-1 expression in oligodendrocytes led to a loss in both glycolytic and mitochondrial metabolism in oligodendrocytes. Therefore, SHP-1 expression in oligodendrocytes is critical for maintaining normal bioenergetics in oligodendrocytes. Because we determined that SHP-1 controls STAT1 signaling in oligodendrocytes, and increased STAT1 correlated with deficient glycolytic and mitochondrial metabolism, we attempted to enhance the metabolic defects in SHP-1-deficient oligodendrocytes by treating SHP-1-deficient mice with IFN-γ for 24 h. After 24 h IFN-γ treatment, there was a significant yet subtle induction in total STAT1 in the oligodendrocytes isolated from these mice (Fig. 6A) but no effects on the induction of Y705-pSTAT3 (Fig. 6B). However, unlike the effects of *in vivo* IFN-γ treatment of wild type mice on downregulating

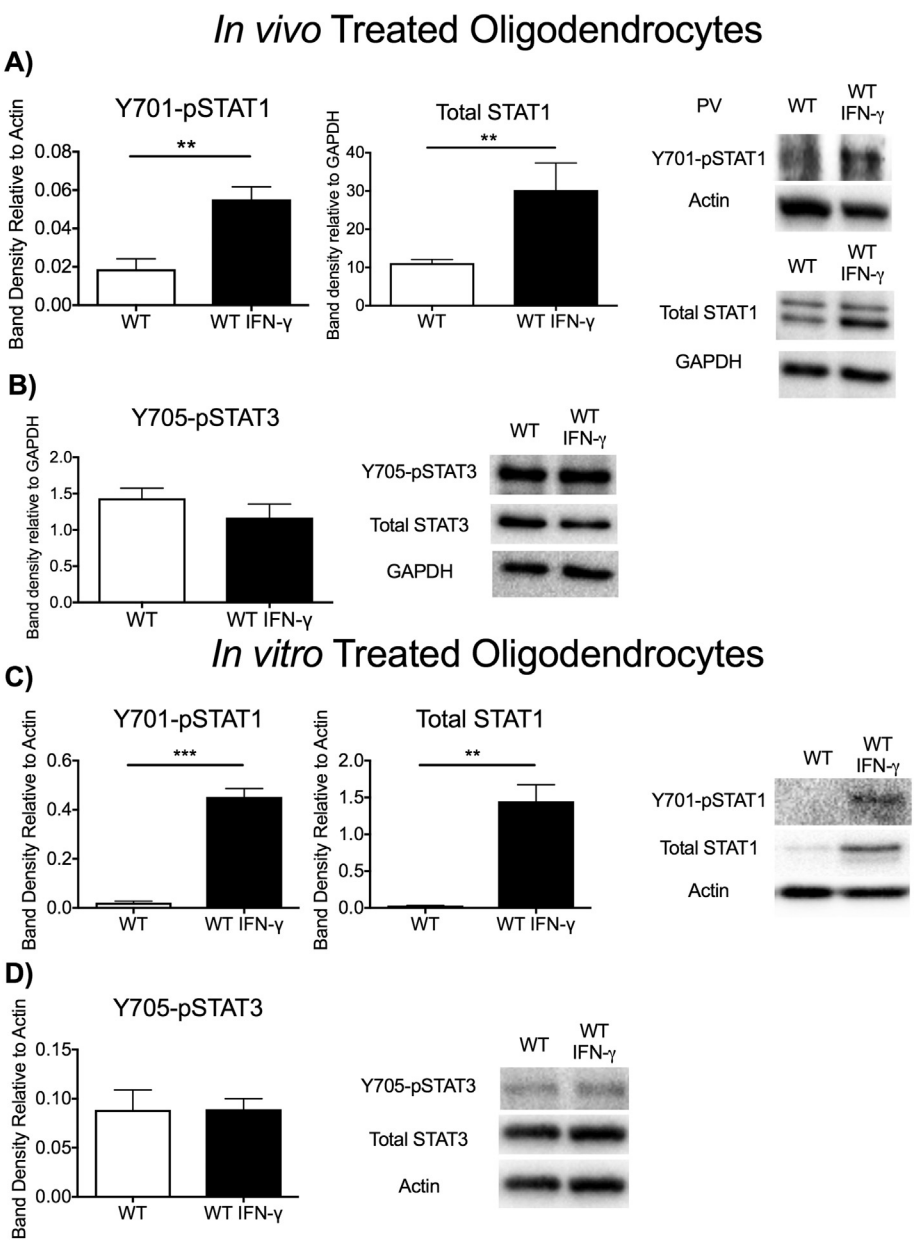

Fig. 3. Constitutive and IFN-γ-inducible STAT1 and Y705-pSTAT3 expression in wild type oligodendrocytes. A) Bar graphs and representative western blots showing Y701-pSTAT1 band density relative to actin ($p = 0.0064$; WT $n = 3$, WT IFN-γ $n = 3$) and total STAT1 relative to GAPDH in oligodendrocytes isolated from untreated wild type (WT) and IFN-γ treated WT mice ($p = 0.0043$; WT $n = 3$, WT IFN-γ $n = 3$). The lysates analyzed for Y701-pSTAT1 were perfused with 100 mM pervanadate (PV) to preserve phosphorylated STAT1, which is highly labile in fresh tissues. B) Bar graph and representative western blot depicting Y705-pSTAT3 band density relative to GAPDH in oligodendrocytes isolated from untreated WT and IFN-γ treated WT mice ($p = 0.1693$; WT $n = 9$, WT IFN-γ $n = 3$). C) Bar graphs and representative western blot showing Y701-pSTAT1 band density relative to actin ($p = 0.0001$; WT $n = 3$, WT IFN-γ $n = 3$) and total STAT1 relative to actin in oligodendrocytes isolated from WT mice and treated *in vitro* with IFN-γ ($p = 0.0016$; WT $n = 3$, WT IFN-γ $n = 3$). D) Bar graph and representative western blot depicting Y705-pSTAT3 band density relative to actin in oligodendrocytes isolated from WT mice and treated *in vitro* with IFN-γ ($p = 0.4870$; WT $n = 3$, WT IFN-γ $n = 3$). Each data point represents oligodendrocytes derived from separate mice. Statistical significance was determined by unpaired one-tailed Student's *t*-test (**$p < 0.01$, ***$p < 0.001$).

oligodendrocyte metabolism (Fig. 1A–H), there were no effects of *in vivo* IFN-γ treatment on SHP-1-deficient oligodendrocytes for all parameters of glycolytic and mitochondrial metabolism (Fig. 7A–H). Based on this outcome, it was concluded that constitutive STAT1 activation in the absence of SHP-1 led to maximal suppression of oligodendrocyte bioenergetics that could not be further suppressed with IFN-γ. The latter supported the hypothesis that SHP-1-deficient cells displayed a constitutive STAT1 activation independent of IFN-γ exposure (Fig. 4A) consistent with constitutively suppressed bioenergetic activities (Fig. 5).

5. Discussion

To our knowledge, we are the first to describe a role for IFN-γ and SHP-1 in the regulation of glycolytic and mitochondrial metabolism in oligodendrocytes as schematically represented in Fig. 8. IFN-γ is known to induce STAT1 transcriptional activity, and relates to previous studies showing that STAT1 impacts aerobic glycolytic and mitochondrial metabolism in a cell type-specific manner that may be either inhibitory or stimulatory (Avalle et al., 2012; Meier and Larner, 2014; Pitroda et al., 2009; Szczepanek et al., 2012; Wong et al., 2002). Here we show that *in vivo* delivery of exogenous IFN-γ impacts oligodendrocytes *via* downregulation of various parameters of both glycolytic and mitochondrial metabolism. We further corroborate this observation in oligodendrocytes of SHP-1-deficient mice which exhibit a constitutive "IFN-γ like state" with increased STAT1 activity and altered bioenergetics independent from exposure to IFN-γ.

In this manuscript, we show a role for IFN-γ in the regulation of metabolism that may provide insight into a potential novel mechanism for the impact of IFN-γ on oligodendrocytes. Besides mature oligodendrocytes, we have considered the possibility that a large proportion of O4-isolated cells from P7 animals may be oligodendrocyte progenitor cells (OPC) and that OPC might contribute in a unique way to the observed bioenergetics profiles in our preparations. As such, bioenergetics measurements of these preparations may be an average between either distinct or similar responses to the treatments. Future experiments will be aimed at separating these populations to characterize their degree of maturational differences with respect to both aerobic glycolysis and mitochondrial respiration. Such differences might reflect on how IFN-γ may affect either maturation of OPC or mature oligodendrocyte

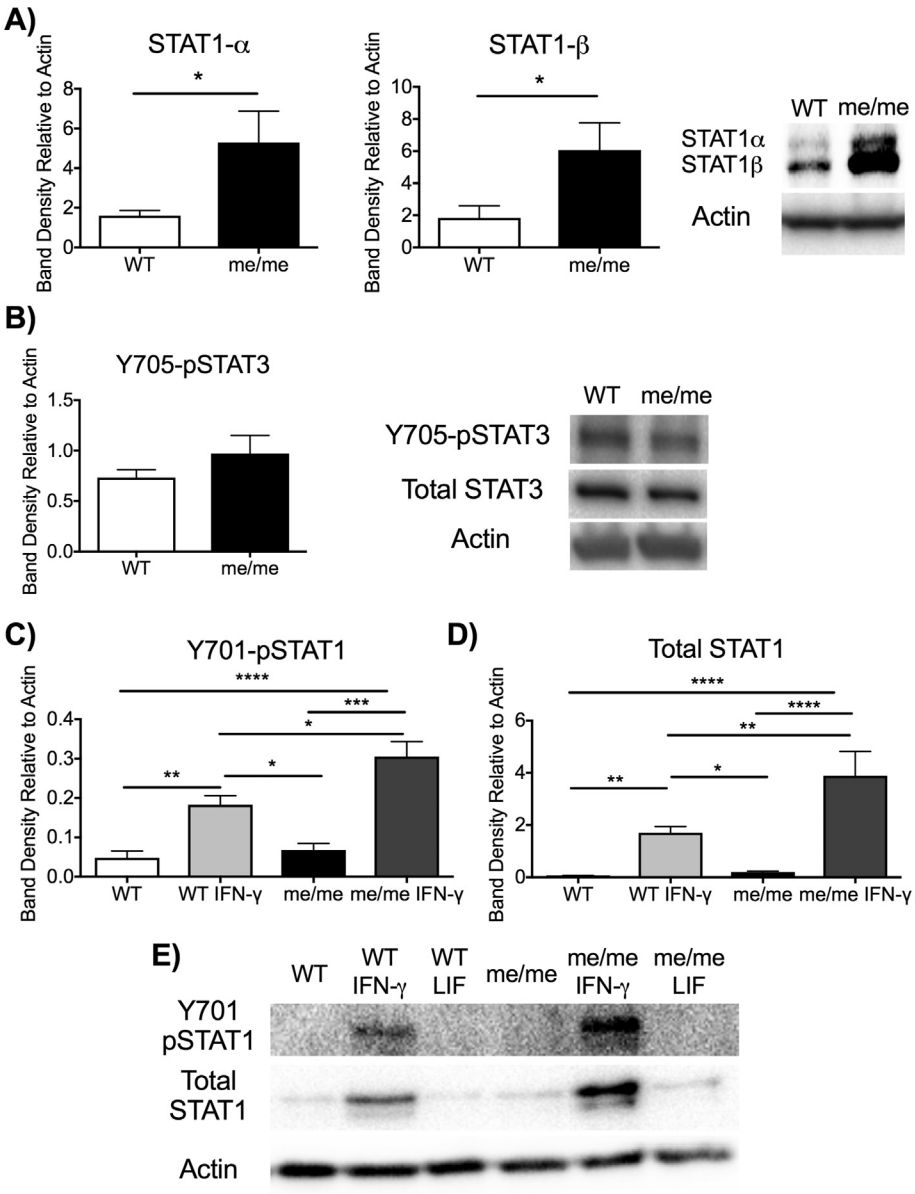

Fig. 4. Constitutive and IFN-γ-inducible STAT1 and Y705-pSTAT3 expression in wild type and SHP-1-deficient oligodendrocytes. A) Bar graphs and representative western blot showing STAT1α and STAT1β band density relative to actin in wild type (WT) and oligodendrocytes from SHP-1 deficient (motheaten, me/me) mice (STAT1α: $p = 0.0306$; WT $n = 4$, me/me $n = 4$; STAT1β: $p = 0.0309$; WT $n = 4$, me/me $n = 4$). B) Bar graph and representative western blot depicting Y705-pSTAT3 band density relative to actin in oligodendrocytes isolated from WT and me/me mice ($p = 0.1157$; WT $n = 4$, me/me $n = 3$). C & D) Bar graphs and E) representative western blots showing inducible C) Y701-pSTAT1 and D) total STAT1 relative to actin in WT and me/me oligodendrocytes treated *in vitro* with either IFN-γ or leukemia inhibitory factor (LIF) relative to untreated oligodendrocytes. Statistical significance was determined by Student's *t*-test or a one-way ANOVA with Tukey's multiple comparisons test (*$p < 0.05$, **$p < 0.01$, ***$p < 0.001$, ****$p < 0.0001$).

functions.

As an approach to demonstrate the effect of IFN-γ on glycolysis and mitochondrial respiration, wild type mice were treated *in vivo* with IFN-γ. IFN-γ specifically induced significant STAT1 activation in wild type mouse oligodendrocytes (Fig. 3A) that was associated with a significant decrease in all measures of oligodendrocyte bioenergetics (Fig. 1A–H). In particular, oligodendrocytes isolated from IFN-γ-treated mice had significantly reduced basal glycolysis (Fig. 1B). Reduced oligodendrocyte basal glycolysis is thought to promote cell survival at the cost of myelination as recently described by Antel and coworkers (Rone et al., 2016). Therefore, in the context of neuroinflammation, IFN-γ may be acting *via* bioenergetic alterations to preserve oligodendrocyte survival while inhibiting myelination until the inflammation has resolved. Glycolytic capacity was also significantly reduced in oligodendrocytes after IFN-γ treatment (Fig. 1C) suggesting that IFN-γ may be transcriptionally downregulating glycolytic enzymes. Typically, when glycolysis is inhibited, mitochondrial metabolism will compensate for the reduction in glycolytic metabolism (reverse Warburg effect), however *in vivo* treatment of wild type mice with IFN-γ also elicited a downregulation of all parameters of mitochondrial metabolism (Fig. 1D–H). The IFN-γ-induced reduction of basal mitochondrial oxygen consumption, maximal mitochondrial respiration, mitochondrial ATP production, and spare mitochondrial respiratory capacity (Fig. 1D–H) suggest pathways by which oligodendrocytes may cope with stressful situations related to inflammation and/or remyelination. As the reduction of mitochondrial metabolism in the context of reduced glycolysis was an unexpected result and we did not see this reduction in isolated oligodendrocytes *in vitro*, we presumed that the *in vivo* effects of IFN-γ on mitochondrial function in oligodendrocytes could be indirect *via* the effect of IFN-γ on other CNS cells (Cannella and Raine, 2004). We hypothesize that the reduction of mitochondrial metabolism can be attributed to inducible nitric oxide synthase (iNOS) induced by IFN-γ in astrocytes and microglia (Tran et al., 2000) which would increase nitric oxide (NO) levels in the CNS leading to nitrosylation and inhibition of the electron transport chain (ETC) (Heales et al., 1999) (Fig. 8). Since oligodendrocytes provide a major energy source to axons in the form of lactate transferred *via* MCT channels (Funfschilling et al., 2012), IFN-γ downregulation of oligodendrocyte mitochondrial metabolism in the context of reduced glycolysis may be a counteractive mechanism to augment lactate levels for use in axonal metabolism under stressful conditions. Our *in vivo* findings likely represent complex interactions between multiple IFN-γ-responsive cells in which the end

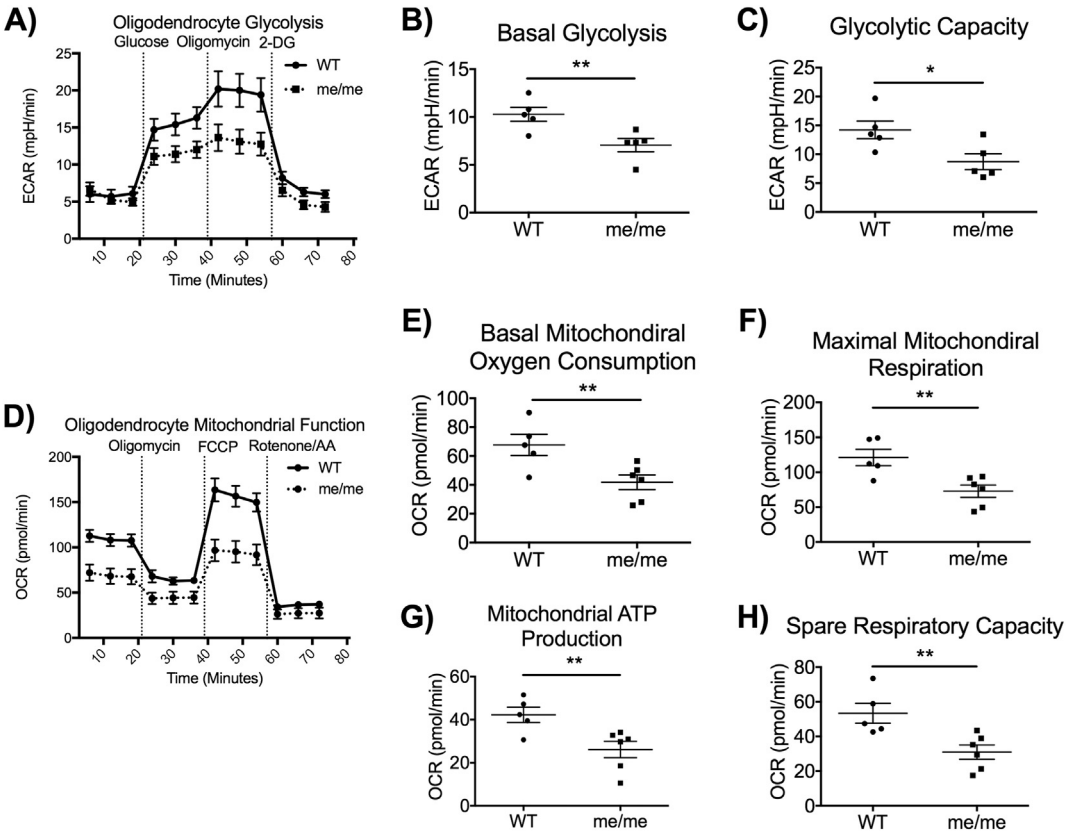

Fig. 5. Constitutive wild type and SHP-1-deficient mouse oligodendrocyte metabolism. A) Seahorse extracellular flux analyzer graph depicting the change in extracellular acidification (ECAR) over time for oligodendrocytes isolated from wild type (WT) and SHP-1 deficient (motheaten, me/me) mice (WT n = 5, me/me n = 5). B & C) Scatter plot graphs depicting B) basal glycolysis ($p = 0.0063$; WT n = 5, me/me n = 5) and C) glycolytic capacity ($p = 0.0284$; WT n = 5, me/me n = 5) from freshly isolated oligodendrocytes isolated from WT and me/me mice. D) Seahorse extracellular flux analyzer graph depicting the oxygen consumption rate (OCR) over time for oligodendrocytes isolated from untreated WT mice and me/me mice (WT n = 4, me/me n = 5). E–H) Scatter plot graphs depicting E) basal mitochondrial oxygen consumption ($p = 0.0077$; WT n = 5, me/me n = 6), F) maximal mitochondrial respiration ($p = 0.0043$; WT n = 5, WT IFN-γ n = 6), G) ATP production ($p = 0.0071$; WT n = 5, WT IFN-γ n = 6), and H) spare respiratory capacity ($p = 0.0051$; WT n = 5, WT IFN-γ n = 6) of oligodendrocytes isolated from WT and me/me mice. Data points are representative of oligodendrocytes isolated from five separate P6-P8 mice and were standardized to GAPDH levels to control for cell numbers between samples. Statistical significance was determined by unpaired one-tailed Student's t-test (*$p < 0.05$, **$p < 0.01$).

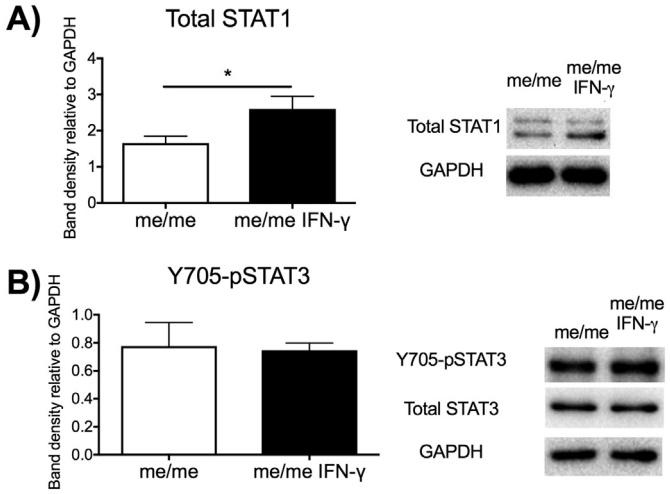

Fig. 6. Total STAT1 and Y705-pSTAT3 expression in oligodendrocytes from SHP-1-deficient mice treated *in vivo* with IFN-γ. A) Bar graph and representative western blot showing total STAT1 band density relative to GAPDH in oligodendrocytes isolated from untreated and IFN-γ treated SHP-1-deficient (motheaten, me/me) mice ($p = 0.0284$; me/me n = 4, me/me IFN-γ n = 4). B) Bar graph and representative western blot depicting Y705-pSTAT3 relative to GAPDH in oligodendrocytes isolated from untreated me/me mice and IFN-γ-treated me/me mice ($p = 0.4489$; me/me n = 5, me/me IFN-γ n = 3). Data points depict oligodendrocytes isolated from the brains and spinal cords of individual animals. Statistical significance was determined by unpaired one-tailed Student's t-test (*$p < 0.05$).

result on suppressed oligodendrocyte bioenergetics may not strictly extend to whether IFN-γ is either beneficial or detrimental to oligodendrocytes *in vivo* but likely involves other factors including iNOS induced by IFN-γ in the CNS (Tran et al., 2000) (Fig. 8). Additionally, the role of IFN-γ on induction of antiviral state in oligodendrocytes has been demonstrated which may be beneficial or detrimental in controlling virus-induced demyelinating disease caused by oligodendrocyte-tropic viruses (Bergmann et al., 2003; De-Simone et al., 2015; Gonzalez et al., 2005; Parra et al., 2010; Schijns et al., 1991; Tsunoda et al., 2006). Of particular interest, the present studies may relate to a novel mechanism of antiviral state induced by IFN-γ in oligodendrocytes as numerous viruses rely on aerobic glycolysis for efficient replication (Allonso et al., 2015; Findlay and Ulaeto, 2015; Fontaine et al., 2015; Liu et al., 2015; Ma et al., 2015; Sanchez and Lagunoff, 2015).

Based on previous studies in our laboratory on the role of SHP-1 on oligodendrocyte biology, we favor the possibility that increased IFN-γ, STAT1, and reduced bioenergetics especially in the context of SHP-1-deficiency may be directly detrimental to oligodendrocytes by various mechanisms including apoptosis. For instance, the induction of the STAT1 responsive genes by IFN-γ has also been shown to promote apoptosis in both mature oligodendrocytes (Agresti et al., 1998; Balabanov et al., 2006; Buntinx et al., 2004) and oligodendrocyte progenitor cells (OPC) (Tirotta et al., 2011). We envision that severe bioenergetics suppression may augment cytotoxic effects of IFN-γ in oligodendrocytes. Having stated this, the effect of IFN-γ on oligodendroyctes is complex with regard to apoptosis and cell survival as IFN-γ

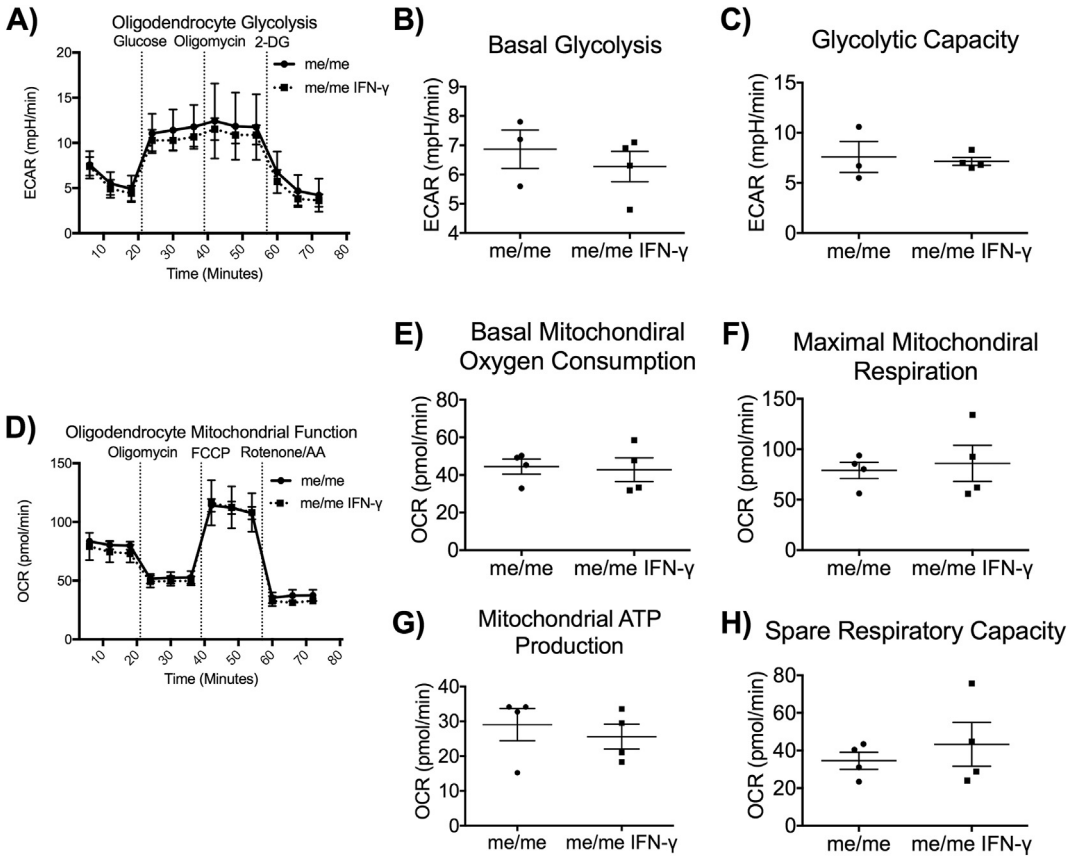

Fig. 7. Constitutive and *in vivo* IFN-γ-treated SHP-1-deficient oligodendrocyte metabolism. A) Seahorse extracellular flux analyzer graph depicting the change in extracellular acidification (ECAR) over time for oligodendrocytes isolated from untreated SHP-1-deficient (motheaten, me/me) mice and IFN-γ me/me mice (me/me n = 4, me/me IFN-γ n = 4). B & C) Scatter plot graphs depicting B) basal glycolysis (p = 0.2572; me/me n = 3, me/me IFN-γ n = 4) and C) glycolytic capacity (p = 0.3780; me/me n = 3, me/me-γ n = 4) of oligodendrocytes from untreated me/me mice and me/me mice treated with IFN-γ. D) Seahorse extracellular flux analyzer graph depicting the oxygen consumption rate (OCR) over time for oligodendrocytes isolated from untreated me/me mice, and me/me mice treated with IFN-γ (me/me n = 4, me/me IFN-γ n = 4). E-H) Scatter plot graphs depicting E) basal mitochondrial oxygen consumption (p = 0.4188; me/me n = 4, me/me IFN-γ n = 4), F) maximal mitochondrial respiration (p = 0.3649; me/me n = 4, me/me IFN-γ n = 4), G) ATP production (p = 0.2879; me/me n = 4, me/me IFN-γ n = 4), and H) spare respiratory capacity (p = 0.2563; me/me n = 4, me/me IFN-γ n = 4) of oligodendrocytes isolated from untreated and IFN-γ treated me/me mice. Graphs depict oligodendrocytes isolated from the brains and spinal cords of P7-P8 mice, standardized to GAPDH levels to control for cell numbers between samples. Each data point represents oligodendrocytes derived from a single mouse and significance was determined by unpaired one-tailed Student's t-test.

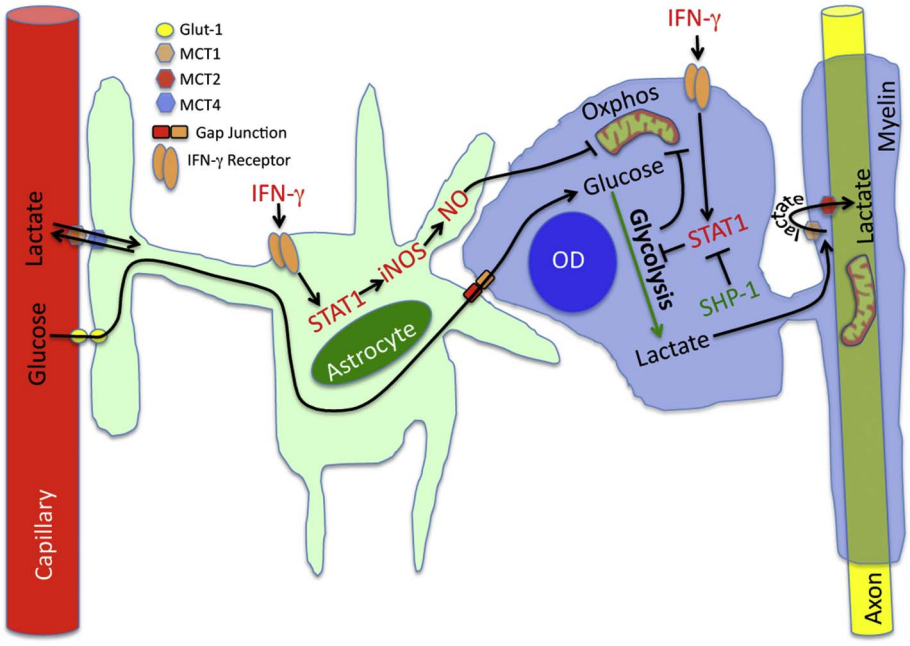

Fig. 8. Schematic diagram of potential pathways by which IFN-γ and SHP-1 regulate oligodendrocyte glycolytic and mitochondrial metabolism. *In vivo* action of IFN-γ or SHP-1 deficiency in oligodendrocytes leads to heightened STAT1 activity that correlates with reduced glycolysis. Reduced glycolysis would reduce the amount of lactate produced, however, mitochondrial metabolism is also reduced in oligodendrocytes thus sparing lactate for use in axonal mitochondria metabolism *via* transfer through monocarboxylate transporters (MCT) MCT1 and MCT2 channels located on the myelin membrane and axonal membrane respectively (Funfschilling et al., 2012; Rinholm et al., 2011). Direct signaling of IFN-γ on oligodendrocytes *in vitro* resulted in reduced glycolysis, however we propose that mitochondrial metabolism is reduced by other pathways stimulated by IFN-γ *in vivo*. One likely indirect effect of IFN-γ on oligodendrocytes only seen *in vivo* is the induction of inducible nitric oxide synthase (iNOS) by astrocytes which then secrete NO in the vicinity of oligodendrocytes (Tran et al., 2000). NO is known to downregulate mitochondrial respiration (Heales et al., 1999) which may preserve lactate levels to mitigate direct effects of IFN-γ on glycolysis in oligodendrocytes and preserve axonal function during inflammatory disease.

has been shown to protect against oligodendrocyte apoptosis and demyelination in experimental autoimmune encephalitis in mice (Balabanov et al., 2007) indicating that some degree of bioenergetics suppression may be protective against oligodendrocyte toxicity and dysfunction as proposed recently (Rone et al., 2016). As a possible mechanism of IFN-γ-induced apoptosis related to the present studies, the reduced activity of aerobic glycolysis by IFN-γ would affect both ATP production and flux through the associated pentose phosphate pathway (PPP) leading to a depletion of reduced glutathione (GSH) and consequent oxidative damage to oligodendrocyte mitochondria. Such damage and ATP depletion has been shown to cause cytochrome C leakage into the cytoplasm and induction of the intrinsic apoptotic pathway (Garcia-Perez et al., 2012; Garedew et al., 2010; Watanabe et al., 2003).

To verify that IFN-γ signaled into oligodendrocytes, STAT1 phosphorylation and expression were measured. STAT1 transcriptionally autoregulates its own expression (Wong et al., 2002) and thus increased total STAT1 in IFN-γ treated wild type oligodendrocytes coincides with increased Y701-pSTAT1 (Fig. 3A,C). Throughout this study, activated STAT3 (Y705-pSTAT3) was used as a control since "cross-talk" between IFN-γ-induced STAT1 signaling may occur *via* SOCS3 mediated downregulation of Y705-STAT3. Thus, it was important to show specificity for IFN-γ signaling in oligodendrocytes, especially in the context of SHP-1 deficiency. We observed a strong correlation between the induction of STAT1 and metabolic alterations in oligodendrocytes. Therefore, it is feasible that IFN-γ may be exerting its effects on oligodendrocyte metabolism through STAT1 transcriptional activity. Metabolic regulation by STAT1 has been previously described in other cell types and it is possible that this may be the mechanism behind IFN-γ induced metabolic alterations of oligodendrocytes (David et al., 1995; Hiroi et al., 2009; Pitroda et al., 2009; Ramana et al., 2000; Sisler et al., 2015).

Oligodendrocytes from SHP-1-deficient (motheaten, me/me) mice were analyzed since SHP-1 is a major negative regulator of IFN-γ signaling in CNS glia (Massa and Wu, 1996). Oligodendrocytes isolated from SHP-1-deficient mice had significantly higher constitutive STAT1 activation (Fig. 4A), but no significant differences in STAT3 activation compared to those of wild type mice (Fig. 4B). Previous research has determined that SHP-1-deficient cells have deranged IFN signaling and therefore respond to IFN-α and IFN-β the same way they respond to IFN-γ with increased STAT1 homodimer activation (David et al., 1995). This makes it highly likely that the constitutively elevated STAT1 in SHP-1-deficient oligodendrocytes represents STAT1 in an "IFN-γ like state". Further, the induction of Y701-pSTAT1 and total STAT1 after IFN-γ treatment were significantly higher in SHP-1-deficient oligodendrocytes relative to IFN-γ-treated wild type oligodendrocytes (Fig. 4C–E), thus demonstrating a direct role for SHP-1 in controlling IFN-γ signaling in oligodendrocytes. High STAT1 correlated with reduced parameters of glycolytic and mitochondrial metabolism in SHP-1-deficient oligodendrocytes (Fig. 5A–H) and recapitulated the metabolic alterations described in wild type oligodendrocytes treated with IFN-γ (Fig. 1A–H). Surprisingly, IFN-γ did not have any effects on glycolytic or mitochondrial metabolism in oligodendrocytes isolated from SHP-1-deficient mice (Fig. 7A–H) even though IFN-γ significantly increased total STAT1 expression (Fig. 6A). We attribute this unexpected result to the constitutive "IFN-γ like state" already established by the significantly higher STAT1 levels in SHP-1-deficient oligodendrocytes (Fig. 4A). Therefore, SHP-1-deficient oligodendrocytes may be maximally metabolically repressed rendering the excess total STAT1 induced by IFN-γ ineffective in further reducing metabolism.

Defects in glycolytic and mitochondrial metabolism can cause deficits in myelination since lipid synthesis is highly dependent upon metabolites generated by both glycolysis and the mitochondria. We have previously demonstrated that white matter tracts in the CNS of SHP-1-deficient mice display dysmyelination and oligodendrocyte abnormalities (Massa et al., 2000; Massa et al., 2004). We propose that defects in SHP-1-deficient oligodendrocyte glycolytic and mitochondrial metabolism are major factors driving dysmyelination in these mice. In support, oligodendrocytes are dependent on adequate metabolic function to properly myelinate axons and maintain myelin sheathes after myelination has occurred (Funfschilling et al., 2012). To explain this dependence, mitochondrial respiration, glycolysis and the associated PPP are critical in providing both large amounts of ATP and metabolites for the proliferation of oligodendrocyte progenitors and the synthesis of myelin lipids and proteins during active myelination (Steiner et al., 2014; Sykes et al., 1986). Recent work has addressed possible relevance of glycolysis in demyelinating disease in which heightened glycolysis promoted process extension as a measure of myelination and lowered aerobic glycolysis was shown to promote process retraction and oligodendrocyte survival that may be relevant to the human demyelinating disease multiple sclerosis (Rone et al., 2016). The later may relate to circumstance where IFN-γ has been shown to be beneficial to oligodendrocytes in experimental autoimmune encephalomyelitis, an important animal model for MS (Balabanov et al., 2007). The authors also showed that aerobic glycolysis was especially high in oligodendrocyte progenitors relative to mature oligodendrocytes indicating the importance of glycolysis in oligodendrocyte proliferation and myelin membrane formation. Thus, the study of glycolytic and mitochondrial metabolism is relevant for a better understanding of demyelinating diseases. Further, adequate oligodendrocyte glycolytic function is required to maintain axonal energy demands because lactate, a byproduct of glycolysis in oligodendrocytes, is necessary to support axonal mitochondrial oxidative phosphorylation (Lee et al., 2012). Therefore, oligodendrocyte metabolic dysfunction may also contribute to axonal energy failure and eventually axonal degeneration. Understanding how SHP-1 regulates metabolic function in oligodendrocytes may further explain how these metabolic derangements occur.

6. Conclusions

Understanding how proinflammatory cytokines such as IFN-γ modulate metabolism is likely to be relevant to both autoimmune and virus-induced oligodendrocyte pathology and demyelinating diseases. Heretofore, IFN-γ was thought to induce oligodendrocyte pathology and demyelination by invoking a proinflammatory process that includes mobilization of myeloid cells against myelin and production of noxious molecules that damage oligodendrocytes (Corbin et al., 1996; Horwitz et al., 1997). It is plausible that IFN-γ may act directly on oligodendrocytes to alter bioenergetics in way not compatible with their role in both myelination and supportive functions for axons. Alternatively, many groups have reported that IFN-γ is protective in the context demyelinating processes such as EAE or virus-induced demyelination, which may be attributed to the ability of IFN-γ to downregulate oligodendrocyte metabolism in such a way as to maintain reduced virus replication and/or promote oligodendrocyte survival (Rone et al., 2016; Willenborg et al., 1996). Thus, the present observations suggest novel ways by which IFN-γ and SHP-1 may exert effects on CNS white matter by altering oligodendrocyte bioenergetics that affect either oligodendrocyte viability or pathology in a context-specific manner.

Supplementary data to this article can be found online at https://doi.org/10.1016/j.jneuroim.2017.10.015.

Acknowledgements

We thank Daria LaRocca, Ross Gruber, Ph.D., and Anthony Paredes for their help with the isolation of oligodendrocytes. We also thank Wanda Coombs and Steven Taffet, Ph.D. for their help with western immunoblotting and scientific discussion. This work was supported by R01NS073810 to PTM and F30NS095498 to SBM. The authors declare that the research was conducted in the absence of any commercial or financial relationships that could be construed as a potential conflict of

interest.

References

Agresti, C., Bernardo, A., Del Russo, N., Marziali, G., Battistini, A., Aloisi, F., Coccia, E.M., 1998. Synergistic stimulation of MHC class I and IRF-1 gene expression by IFN-gamma and TNF-alpha in oligodendrocytes. Eur. J. Neurosci. 10, 2975–2983.

Allonso, D., Andrade, I.S., Conde, J.N., Coelho, D.R., Rocha, D.C., da Silva, M.L., Ventura, G.T., Silva, E.M., Mohana-Borges, R., 2015. Dengue virus NS1 protein modulates cellular energy metabolism by increasing glyceraldehyde-3-phosphate dehydrogenase activity. J. Virol. 89, 11871–11883.

Amaral, A.I., Meisingset, T.W., Kotter, M.R., Sonnewald, U., 2013. Metabolic aspects of neuron-oligodendrocyte-astrocyte interactions. Front. Endocrinol. 4, 1–5.

Andrews, H.E., Nichols, P.P., Bates, D., Turnbull, D.M., 2005. Mitochondrial dysfunction plays a key role in progressive axonal loss in Multiple Sclerosis. Med. Hypotheses 64, 669–677.

Avalle, L., Pensa, S., Regis, G., Novelli, F., Poli, V., 2012. STAT1 and STAT3 in tumorigenesis: a matter of balance. Jak-Stat. 1, 65–72.

Balabanov, R., Strand, K., Kemper, A., Lee, J.Y., Popko, B., 2006. Suppressor of cytokine signaling 1 expression protects oligodendrocytes from the deleterious effects of interferon-gamma. J. Neurosci. 26, 5143–5152.

Balabanov, R., Strand, K., Goswami, R., McMahon, E., Begolka, W., Miller, S.D., Popko, B., 2007. Interferon-gamma-oligodendrocyte interactions in the regulation of experimental autoimmune encephalomyelitis. J. Neurosci. 27, 2013–2024.

Bergmann, C.C., Parra, B., Hinton, D.R., Chandran, R., Morrison, M., Stohlman, S.A., 2003. Perforin-mediated effector function within the central nervous system requires IFN-gamma-mediated MHC up-regulation. J. Immunol. 170, 3204–3213.

Bjartmar, C., Trapp, B.D., 2001. Axonal and neuronal degeneration in multiple sclerosis: mechanisms and functional consequences. Curr. Opin. Neurol. 14, 271–278.

Boehm, U., Klamp, T., Groot, M., Howard, J.C., 1997. Cellular responses to interferon-gamma. Annu. Rev. Immunol. 15, 749–795.

Buntinx, M., Gielen, E., Van Hummelen, P., Raus, J., Ameloot, M., Steels, P., Stinissen, P., 2004. Cytokine-induced cell death in human oligodendroglial cell lines. II: alterations in gene expression induced by interferon-gamma and tumor necrosis factor-alpha. J. Neurosci. Res. 76, 846–861.

Cannella, B., Raine, C.S., 2004. Multiple sclerosis: cytokine receptors on oligodendrocytes predict innate regulation. Ann. Neurol. 55, 46–57.

Corbin, J.G., Kelly, D., Rath, E.M., Baerwald, K.D., Suzuki, K., Popko, B., 1996. Targeted CNS expression of interferon-gamma in transgenic mice leads to hypomyelination, reactive gliosis, and abnormal cerebellar development. Mol. Cell. Neurosci. 7, 354–370.

David, M., Chen, H.E., Goelz, S., Larner, A.C., Neel, B.G., 1995. Differential regulation of the alpha/beta interferon-stimulated Jak/Stat pathway by the SH2 domain-containing tyrosine phosphatase SHPTP1. Mol. Cell Biol. 15, 7050–7058.

Decker, T., Kovarik, P., Meinke, A., 1997. GAS elements: a few nucleotides with a major impact on cytokine-induced gene expression. J. Interferon Cytokine Res. 17, 121–134.

De-Simone, F.I., Sariyer, R., Otalora, Y.L., Yarandi, S., Craigie, M., Gordon, J., Sariyer, I.K., 2015. IFN-gamma inhibits JC virus replication in glial cells by suppressing T-antigen expression. PLoS One 10, e0129694.

Findlay, J.S., Ulaeto, D., 2015. Semliki Forest virus and Sindbis virus, but not vaccinia virus, require glycolysis for optimal replication. J. Gen. Virol. 96, 2693–2696.

Fontaine, K.A., Sanchez, E.L., Camarda, R., Lagunoff, M., 2015. Dengue virus induces and requires glycolysis for optimal replication. J. Virol. 89, 2358–2366.

Funfschilling, U., Supplie, L.M., Mahad, D., Boretius, S., Saab, A.S., Edgar, J., Brinkmann, B.G., Kassmann, C.M., Tzvetanova, I.D., Mobius, W., Diaz, F., Meijer, D., Suter, U., Hamprecht, B., Sereda, M.W., Moraes, C.T., Frahm, J., Goebbels, S., Nave, K.A., 2012. Glycolytic oligodendrocytes maintain myelin and long-term axonal integrity. Nature 485, 517–521.

Garcia-Perez, C., Roy, S.S., Naghdi, S., Lin, X., Davies, E., Hajnoczky, G., 2012. Bid-induced mitochondrial membrane permeabilization waves propagated by local reactive oxygen species (ROS) signaling. Proc. Natl. Acad. Sci. U. S. A. 109, 4497–4502.

Garedew, A., Henderson, S.O., Moncada, S., 2010. Activated macrophages utilize glycolytic ATP to maintain mitochondrial membrane potential and prevent apoptotic cell death. Cell Death Differ. 17, 1540–1550.

Gonzalez, J.M., Bergmann, C.C., Fuss, B., Hinton, D.R., Kangas, C., Macklin, W.B., Stohlman, S.A., 2005. Expression of a dominant negative IFN-gammareceptor on mouse oligodendrocytes. Glia 51, 22–34.

Goverman, J., 2009. Autoimmune T cell responses in the central nervous system. Nat Rev Immunol. 9, 393–407.

Gruber, R.C., LaRocca, D., Minchenberg, S.B., Christophi, G.P., Hudson, C.A., Ray, A.K., Shafit-Zagardo, B., Massa, P.T., 2015. The control of reactive oxygen species production by SHP-1 in oligodendrocytes. Glia 63, 1753–1771.

Heales, S.J., Bolanos, J.P., Stewart, V.C., Brookes, P.S., Land, J.M., Clark, J.B., 1999. Nitric oxide, mitochondria and neurological disease. Biochim. Biophys. Acta 1410, 215–228.

Hiroi, M., Mori, K., Sakaeda, Y., Shimada, J., Ohmori, Y., 2009. STAT1 represses hypoxia-inducible factor-1-mediated transcription. Biochem. Biophys. Res. Commun. 387, 806–810.

Horvat, A., Schwaiger, F.-W., Hager, G., Brocker, F., Streif, R., Knyazev, P.G., Ullrich, A., Kreutzberg, G.W., 2001. A novel role for protein tyrosine phosphatase SHP1 in controlling glial activation in the normal and injured nervous system. J. Neurosci. 21, 865–874.

Horwitz, M.S., Evans, C.F., McGavern, D.B., Rodriguez, M., Oldstone, M.B.A., 1997. Primary demyelination in transgenic mice expressing interferon-gamma. Nat. Med. 3, 1037–1041.

Karhumaki, E., Helin, H., 1987. Regulation of oxidative metabolism by interferon-gamma during human monocyte to macrophage differentiation. Med. Biol. 65, 261–266.

Lee, Y., Morrison, B.M., Li, Y., Lengacher, S., Farah, M.H., Hoffman, P.N., Liu, Y., Tsingalia, A., Jin, L., Zhang, P.W., Pellerin, L., Magistretti, P.J., Rothstein, J.D., 2012. Oligodendroglia metabolically support axons and contribute to neurodegeneration. Nature 487, 443–448.

Lees, J.R., Cross, A.H., 2007. A little stress is good: IFN-gamma, demyelination, and multiple sclerosis. J. Clin. Invest. 117, 297–299.

Lin, W., Kemper, A., Dupree, J.L., Harding, H.P., Ron, D., Popko, B., 2006. Interferon-gamma inhibits central nervous system remyelination through a process modulated by endoplasmic reticulum stress. Brain 129, 1306–1318.

Lin, W., Bailey, S.L., Ho, H., Harding, H.P., Ron, D., Miller, S.D., Popko, B., 2007. The integrated stress response prevents demyelination by protecting oligodendrocytes against immune-mediated damage. J. Clin. Invest. 117, 448–456.

Liu, B., Fang, M., He, Z., Cui, D., Jia, S., Lin, X., Xu, X., Zhou, T., Liu, W., 2015. Hepatitis B virus stimulates G6PD expression through HBx-mediated Nrf2 activation. Cell Death Dis. 6, e1980.

Loda, E., Balabanov, R., 2012. Interferon regulatory factor 1 regulation of oligodendrocyte injury and inflammatory demyelination. Rev. Neurosci. 23, 145–152.

Ma, T., Patel, H., Babapoor-Farrokhran, S., Franklin, R., Semenza, G.L., Sodhi, A., Montaner, S., 2015. KSHV induces aerobic glycolysis and angiogenesis through HIF-1-dependent upregulation of pyruvate kinase 2 in Kaposi's sarcoma. Angiogenesis 18, 477–488.

Mahad, D.J., Ziabreva, I., Campbell, G., Lax, N., White, K., Hanson, P.S., Lassmann, H., Turnbull, D.M., 2009. Mitochondrial changes within axons in multiple sclerosis. Brain 132, 1161–1174.

Massa, P.T., Wu, C., 1996. The role of protein tyrosine phosphatase SHP-1 in the regulation of IFN-gamma signaling in neural cells. J. Immunol. 157, 5139–5144.

Massa, P.T., Saha, S., Wu, C., Jarosinski, K.W., 2000. Expression and function of the protein tyrosine phosphatase SHP-1 in oligodendrocytes. Glia 29, 376–385.

Massa, P.T., Wu, C., Fecenko-Tacka, K., 2004. Dysmyelination and reduced myelin basic protein gene expression by oligodendrocytes of SHP-1-deficient mice. J. Neurosci. Res. 77, 15–25.

Meier, J.A., Larner, A.C., 2014. Toward a new STATe: The role of STATs in mitochondrial function. Semin. Immunol. 26, 20–28.

Parra, G.I., Bergmann, C.C., Phares, T.W., Hinton, D.R., Atkinson, R., Stohlman, S.A., 2010. Gamma interferon signaling in oligodendrocytes is critical for protection from neurotropic coronavirus infection. J. Virol. 84, 3111–3115.

Pitroda, S.P., Wakim, B.T., Sood, R.F., Beveridge, M.G., Beckett, M.A., MacDermed, D.M., Weichselbaum, R.R., Khodarev, N.N., 2009. STAT1-dependent expression of energy metabolic pathways links tumour growth and radioresistance to the Warburg effect. BMC Med. 7 (68).

Poli, V., Camporeale, A., 2015. STAT3-mediated metabolic reprograming in cellular transformation and implications for drug resistance. Front. Oncol. 5 (121).

Ramana, C.V., Grammatikakis, N., Chernov, M., Nguyen, H., Goh, K.C., Williams, B.R.G., 2000. Regulation of c-myc expression by IFN-gamma through Stat1-dependent and -independent pathways. EMBO J. 19, 263–272.

Renno, T., Taupin, V., Bourbonniere, L., Verge, G., Tran, E., De Simone, R., Krakowski, M., Rodriguez, M., Peterson, A., Owens, T., 1998. Interferon-gamma in progression to chronic demyelination and neurological deficit following acute EAE. Mol. Cell. Neurosci. 12, 376–389.

Rinholm, J.E., Hamilton, N.B., Kessaris, N., Richardson, W.D., Bergersen, L.H., Attwell, D., 2011. Regulation of oligodendrocyte development and myelination by glucose and lactate. J. Neurosci. 31, 538–548.

Rone, M.B., Cui, Q.L., Fang, J., Wang, L.C., Zhang, J., Khan, D., Bedard, M., Almazan, G., Ludwin, S.K., Jones, R., Kennedy, T.E., Antel, J.P., 2016. Oligodendrogliopathy in multiple sclerosis: low glycolytic metabolic rate promotes oligodendrocyte survival. J. Neurosci. 36, 4698–4707.

Saab, A.S., Tzvetanova, I.D., Nave, K.A., 2013. The role of myelin and oligodendrocytes in axonal energy metabolism. Curr. Opin. Neurobiol. 23, 1065–1072.

Sanchez, E.L., Lagunoff, M., 2015. Viral activation of cellular metabolism. Virology 479-480, 609–618.

Sarafian, T.A., Montes, C., Imura, T., Qi, J., Coppola, G., Geschwind, D.H., Sofroniew, M.V., 2010. Disruption of astrocyte STAT3 signaling decreases mitochondrial function and increases oxidative stress in vitro. PLoS One 5, e9532.

Schijns, V.E., Van der Neut, R., Haagmans, B.L., Bar, D.R., Schellekens, H., Horzinek, M.C., 1991. Tumour necrosis factor-alpha, interferon-gamma and interferon-beta exert antiviral activity in nervous tissue cells. J. Gen. Virol. 72 (Pt 4), 809–815.

Shuai, K., Liu, B., 2003. Regulation of JAK-STAT signalling in the immune system. Nat. Rev. Immunol. 3, 900–911.

Sisler, J.D., Morgan, M., Raje, V., Grande, R.C., Derecka, M., Meier, J., Cantwell, M., Szczepanek, K., Korzun, W.J., Lesnefsky, E.J., Harris, T.E., Croniger, C.M., Larner, A.C., 2015. The signal transducer and activator of transcription 1 (STAT1) inhibits mitochondrial biogenesis in liver and fatty acid oxidation in adipocytes. PLoS One 10, e0144444.

Sosa, R.A., Murphey, C., Robinson, R.R., Forsthuber, T.G., 2015. IFN-gamma ameliorates autoimmune encephalomyelitis by limiting myelin lipid peroxidation. Proc. Natl. Acad. Sci. U. S. A. 112, E5038–5047.

Starr, R., Hilton, D.J., 1999. Negative regulation of the JAK/STAT pathway. BioEssays 21, 47–52.

Steiner, J., Martins-de-Souza, D., Schiltz, K., Sarnyai, Z., Westphal, S., Isermann, B., Dobrowolny, H., Turck, C.W., Bogerts, B., Bernstein, H.G., Horvath, T.L., Schild, L., Keilhoff, G., 2014. Clozapine promotes glycolysis and myelin lipid synthesis in cultured oligodendrocytes. Front. Cell. Neurosci. 8 (384).

Su, X., Yu, Y., Zhong, Y., Giannopoulou, E.G., Hu, X., Liu, H., Cross, J.R., Ratsch, G., Rice,

C.M., Ivashkiv, L.B., 2015. Interferon-gamma regulates cellular metabolism and mRNA translation to potentiate macrophage activation. Nat. Immunol. 16, 838–849.
Sykes, J.E., Lopes-Cardozo, M., Van Den Bergh, S.G., 1986. Relationship between the pentose-phosphate pathway and the de novo synthesis of fatty acids and cholesterol in oligodendrocyte-enriched glial cultures. Neurochem. Int. 8, 77–82.
Szczepanek, K., Lesnefsky, E.J., Larner, A.C., 2012. Multi-Tasking: Nuclear Transcription Factors with Novel Roles in the Mitochondria. Trends Cell Biol. 22, 429–437.
Takikita, S., Takano, T., Narita, T., Maruo, Y., 2015. Increased apoptosis and hypomyelination in cerebral white matter of macular mutant mouse brain. Mol. Genet. Metab. Rep. 4, 25–29.
Tirotta, E., Ransohoff, R.M., Lane, T.E., 2011. CXCR2 signaling protects oligodendrocyte progenitor cells from IFN-gamma/CXCL10-mediated apoptosis. Glia 59, 1518–1528.
Tran, E.H., Prince, E.N., Owens, T., 2000. IFN-gamma shapes immune invasion of the central nervous system via regulation of chemokines. J. Immunol. 164, 2759–2768.
Tsunoda, I., Libbey, J.E., Kobayashi-Warren, M., Fujinami, R.S., 2006. IFN-gamma production and astrocyte recognition by autoreactive T cells induced by Theiler's virus infection: role of viral strains and capsid proteins. J. Neuroimmunol. 172, 85–93.
Valentino, L., Pierre, J., 2006. JAK/STAT signal transduction: regulators and implication in hematological malignancies. Biochem. Pharmacol. 71, 713–721.
Vartanian, T., Li, Y., Zhao, M., Stefansson, K., 1995. Interferon-gamma-induced oligodendrocyte cell death: implications for the pathogenesis of multiple sclerosis. Mol. Med. 1, 732–743.
Watanabe, Y., Suzuki, O., Haruyama, T., Akaike, T., 2003. Interferon-gamma induces reactive oxygen species and endoplasmic reticulum stress at the hepatic apoptosis. J. Cell. Biochem. 89, 244–253.
Wegrzyn, J., Potla, R., Chwae, Y.J., Sepuri, N.B., Zhang, Q., Koeck, T., Derecka, M., Szczepanek, K., Szelag, M., Gornicka, A., Moh, A., Moghaddas, S., Chen, Q., Bobbili, S., Cichy, J., Dulak, J., Baker, D.P., Wolfman, A., Stuehr, D., Hassan, M.O., Fu, X.Y., Avadhani, N., Drake, J.I., Fawcett, P., Lesnefsky, E.J., Larner, A.C., 2009. Function of mitochondrial Stat3 in cellular respiration. Science 323, 793–797.
Willenborg, D.O., Fordham, S., Bernard, C.C., Cowden, W.B., Ramshaw, I.A., 1996. IFN-gamma plays a critical down-regulatory role in the induction and effector phase of myelin oligodendrocyte glycoprotein-induced autoimmune encephalomyelitis. J. Immunol. 157, 3223–3227.
Wishcamper, C.A., Coffin, J.D., Lurie, D.I., 2001. Lack of the protein tyrosine phosphatase SHP-1 results in decreased numbers of glia within the motheaten (me/me) mouse brain. J. Comp. Neurol. 441, 118–133.
Wong, L.H., Sim, H., Chatterjee-Kishore, M., Hatzinisiriou, I., Devenish, R.J., Stark, G., Ralph, S.J., 2002. Isolation and characterization of a human STAT1 gene regulatory element. Inducibility by interferon (IFN) types I and II and role of IFN regulatory factor-1. J. Biol. Chem. 277, 19408–19417.
Ziabreva, I., Campbell, G., Rist, J., Zambonin, J., Rorbach, J., Wydro, M.M., Lassmann, H., Franklin, R.J., Mahad, D., 2010. Injury and differentiation following inhibition of mitochondrial respiratory chain complex IV in rat oligodendrocytes. Glia 58, 1827–1837.